Journal of Pediatric Surgery 55 (2020) 1621–1625

Contents lists available at ScienceDirect

Journal of Pediatric Surgery

journal homepage: www.elsevier.com/locate/jpedsurg

Altered anoctamin-1 and tyrosine phosphorylation in congenital ureteropelvic junction obstruction

Manuela Hunziker [a,b], Anne-Marie O'Donnell [a], Jan Gosemann [a], Luis A. Alvarez [a], Prem Puri [a,b,*]

[a] National Children's Research Centre, Our Lady's Children's Hospital, Dublin, Ireland
[b] School of Medicine and Medical Science and Conway Institute of Biomolecular and Biomedical Research, University College Dublin, Ireland

ARTICLE INFO

Article history:
Received 4 June 2019
Received in revised form 26 November 2019
Accepted 5 February 2020

Key words:
Ureteropelvic junction
Kidney
Peristalsis
Anoctamin 1

ABSTRACT

Purpose: Ureteropelvic junction (UPJ) obstruction is the most common cause of congenital hydronephrosis in children. The pathophysiology of UPJ obstruction and the exact mechanism of pelviureteral peristalsis are poorly understood. Anoctamin-1 (ANO1), a Ca^{2+}-activated chloride channel, has been shown to play a key role in muscle wall contractions in the gastrointestinal tract. We designed this study to investigate the hypothesis that ANO1 is expressed in smooth muscle cells (SMCs) of the human UPJ and that tyrosine phosphorylation is altered in UPJ obstruction.

Materials and methods: Fresh frozen specimens of UPJ obstruction ($n = 28$) and control specimens from patients who underwent Wilms' tumor nephrectomy ($n = 20$) were prepared. Western blot (WB) was performed to evaluate levels of ANO1 protein expression and changes in tyrosine phosphorylation. In addition analysis of ANO1 and phalloidin using confocal-immunofluoresence-double staining and 3D reconstruction were carried out.

Results: Our WB results revealed increased tyrosine phosphorylation in UPJ obstruction samples compared to controls, and decreased ANO1 expression in UPJ obstruction. Confocal microscopy showed that ANO1 immunoreactivity was decreased in SMCs of UPJ obstruction compared to controls.

Conclusions: We provide evidence, for the first time, of the presence of ANO1 expression in the human UPJ. We speculate that altered tyrosine phosphorylation, observed in UPJ obstruction, may lead to a failure of transmission of peristaltic waves in UPJ obstruction by inhibiting Ca^{2+}-activated chloride channels in SMCs.

The unique function of the upper urinary tract is to propel urine from the kidney into the ureter and bladder for storage until micturition [1]. The cellular mechanisms which underlie the initiation and propagation of the peristaltic contractions remain poorly understood [1]. It is believed that coordinated contractions of SMCs produce motor patterns for transmission of peristaltic waves across the UPJ. In UPJ obstruction, disruption of the coordinated motion of SMCs may result in impaired peristalsis [2] leading to the accumulation of urine in the kidney and dilatation of the renal pelvis.

Anoctamin-1 (ANO1) is a Ca^{2+}-activated chloride channel which plays a multitude of important physiological functions including smooth muscle contraction, transepithelial ion transport, and regulation of neuronal excitability and vascular tone. Expression of ANO1 has been described in the smooth muscle cells (SMCs) of the murine renal pelvis [3], urethra of mice, rats and sheep [4] and urinary bladder of the rat [5].

A source of complexity influencing the role of ANO1 in SMCs is phosphorylation [6]. It has been shown that ANO1 undergoes a reorganization of its structure and function by posttranslational modifications such as phosphorylation. Phosphorylation on tyrosine residues can modify channel activity and alter electrophysiological properties of excitable cells [7]. In particular in SMCs, phosphorylation has been shown to inhibit Ca^{2+}-activated chloride channels [8]. We designed this study to investigate the hypothesis that ANO1 is expressed in SMCs of the human UPJ and that tyrosine phosphorylation is altered in UPJ obstruction.

1. Materials and methods

This study was approved by the Ethics (Medical Research) Committee, Our Lady's Children's Hospital, Dublin (Ref. GEN/200/11) and tissue samples were obtained with informed patient consent. UPJ specimens from 28 patients with a mean age of 1.3 years (3 months to 3.3 years) who underwent pyeloplasty for intrinsic UPJ obstruction were studied. Extrinsic UPJ obstruction cases were excluded from the study. Control samples included 20 UPJ specimens from patients who underwent Wilms' tumor nephrectomy with a mean age of 2.4 years (4 months to 4.8 years). Tissue 1.5 cm from the UPJ region containing the UPJ was resected from control and UPJ obstruction cases. In UPJ controls, we first identified the site where the funnel-shaped renal pelvis became continuous with the ureter and resected 1.5 cm of the UPJ. In UPJ

* Corresponding author at: National Children's Research Centre, Our Lady's Children's Hospital, Dublin, – 12, Ireland. Tel.: +353 1 4096420,
E-mail address: prem.puri@ucd.ie (P. Puri).

https://doi.org/10.1016/j.jpedsurg.2020.02.001
0022-3468/

obstruction cases, the junction was easier to identify owing to the abrupt luminal narrowing of the pelvis and 1.5 cm of UPJ were obtained. Specimens were either snap-frozen in liquid nitrogen or stored at −80 °C for RNA and protein extraction or embedded in OCT Mounting Compound (VWR International, Leuven, Belgium) and stored at −80 °C for immunofluorescence staining.

1.1. RNA isolation

Total RNA was isolated using the Qiagen miRNeasy Mini Kit (Qiagen Ltd., Manchester, UK) according to the manufacturer's protocol. Spectrophotometrical quantification of total RNA was performed (NanoDrop ND-1000 UV–Vis Spectrophotometer) and the RNA was stored at −80 °C.

1.2. cDNA synthesis and quantitative polymerase chain reaction

Reverse transcription of total RNA was carried out at 85 °C for 3 min (denaturation), at 44 °C for 60 min (annealing) and at 92 °C for 10 min (reverse transcriptase inactivation), using Transcriptor High Fidelity cDNA Synthesis Kit (Roche Diagnostics, Germany) according to the manufacturer's instructions. Resulting cDNA was used for quantitative real-time polymerase chain reaction (qRT-PCR) using a LightCycler 480 SYBR Green I Master (Roche Diagnostics, Germany) in a total reaction mix of 20 μl per well. A total of 16 UPJ samples and 8 control samples were used for RT-PCR. RT-PCR was performed in triplicate. RT-PCR was performed using specific primers designed from known ANO1 sequences, directed against regions of the mRNA. A gene-specific primer pair, ANO1 forward 5′-GGGCTTTGAAGAGGAAGAGG-3′ and reverse 5′-TCTCCAAGACTCTGGCTTCG-3′, was designed based on the published ANO1 transcript sequence (GeneBank accession number: NM-018043), yielding a predicted 71 bp amplicon. After 5 min of initial denaturation at 95 °C, 45 cycles of amplification for each primer were carried out. Each cycle included denaturation at 95 °C for 10 s, annealing at 60 °C for 15 s, and elongation at 72 °C for 10 s. Relative levels of gene expression were determined using a LightCycler 480 (Roche Diagnostics, Germany) and the relative changes in expression levels of ANO1 were normalized against the level of GAPDH gene expression in each sample ($\Delta\Delta C_T$-method) (GAPDH forward primer 5′-GGAGTCAACGGATTTGGT-3′ and GAPDH reverse 5′-GTGATGGGATTTCCATTGAT-3′). Experiments were carried out in duplicate for each sample and primer.

1.3. Western blot

A total of 9 obstructed UPJ and 9 control UPJ specimens were homogenized in RIPA buffer (Radio Immunoprecipitation Assay from Sigma-Aldrich, Ireland) containing 1% protease inhibitor cocktail (Sigma-Aldrich Ltd., Ireland). Protein concentrations were determined using a Bradford assay (Sigma-Aldrich Ltd., Ireland). 20 μl Laemmli sample buffer (Sigma-Aldrich Ireland Ltd., Ireland) containing 10 μg of protein was loaded in the 10% SDS-PAGE gel (NuPAGE Novex Bis–Tris gels, Invitrogen, UK) for electrophoretic separation. The electrophoresis was performed in MES SDS running buffer (Invitrogen, UK). Proteins were then transferred to 0.45 μm nitrocellulose membrane (Millipore Corporation, USA) by western blotting. Primary antibodies against ANO1 (rabbit polyclonal, ab53212 dilution 1:500, Abcam, UK) and p-Tyro (mouse monoclonal, sc-7020, dilution 1:1000, Santa Cruz Biotechnology Inc., Germany) were used and incubation was performed overnight at 4 °C. Membranes were incubated with the appropriate secondary antibodies (goat anti-rabbit IgG, HRP-linked Antibody, 7074S, dilution 1:5000, Cell Signaling Technology-Isis Ltd., Ireland, and goat anti-mouse IgG-HRP, sc-2302, dilution 1:5000, Santa Cruz Biotechnology, Inc., Germany, respectively). Detection was performed with the PIERCE chemiluminescence kit (Thermo, Fisher Scientific, Ireland). We used Anti-ß-actin antibody (ab8227, dilution 1:5000, Abcam, UK) as an additional loading control. Band density was quantified by digital densitometry using the image-analysis software ImageJ. ANO1 and p-Tyro band intensity was normalized to that of β-actin.

Antibody specificity was verified using ANO1 lysates (ANO1 lysates consisting of HEK-293 cells expressing ANO1 tagged on its C terminus with Flag epitopes were a generous gift of H. Chris Hartzell, Emory University, Atlanta, USA).

Table 1
Antibodies and phalloidin used for immunofluorescence.

	Species	Catalogue no.	Dilution	Source
Primary antibodies				
TMEM16 A (ANO1)	Rabbit	ab53212	1:100	Abcam, UK
TMEM16 A (ANO1)	Mouse	Ab190721	1:100	Abcam, UK
c-kit	Rabbit	A4502	1:100	Dako, Denmark
c-kit	Mouse	ab52559	1:100	Abcam, UK
Secondary antibodies			1:500	
Alexa Fluor 488 donkey anti-mouse IgG		ab150109	1:500	Abcam, UK
Alexa Fluor 647 donkey anti-rabbit IgG		ab150067	1:500	Abcam, UK
Phalloidin				
Alexa Fluor Phalloidin 488		A12379	1:500	Invitrogen, UK
Alexa Fluor Phalloidin 635		A34054	1:500	Invitrogen, UK

1.4. Immunofluorescence double staining and confocal microscopy

A total of 3 frozen blocks of UPJ obstruction and 3 UPJ control samples frozen blocks of UPJ obstruction and UPJ control samples were sectioned transversely at a thickness of 10 μm, mounted on SuperFrost® Plus slides (VWR International, Belgium) and fixed with 10% buffered formalin for 5 min. Information on primary and secondary antibody and Phalloidin sources and concentrations is shown in Table 1. After washing, sections were counterstained with DAPI antibody (10236276001, dilution 1:1000, Roche Diagnostics GmbH, Germany) for 10 min and coverslipped with Fluorescent Mounting Medium (DAKO Ltd., UK). All sections were independently evaluated by two investigators with an LSM 700 confocal microscope (Carl Zeiss MicroImaging GmbH, Germany).

1.5. Statistical analysis

Numerical data are shown as mean ± standard error of the mean (SEM). The statistical significance of difference in ANO1 gene expression levels and the relative density of ANO1 protein and p-Tyro protein

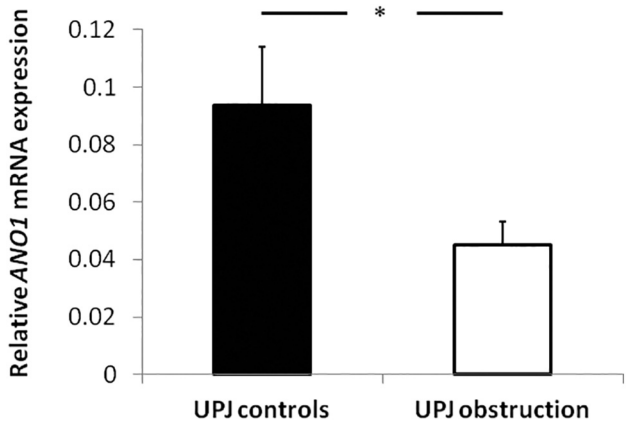

Fig. 1. Relative mRNA expression levels of ANO1 in UPJ controls and UPJ obstruction. The gene expression of ANO1 was significantly decreased (* $p = 0.016$) in UPJ obstruction compared to controls. Results are presented as mean ± SEM.

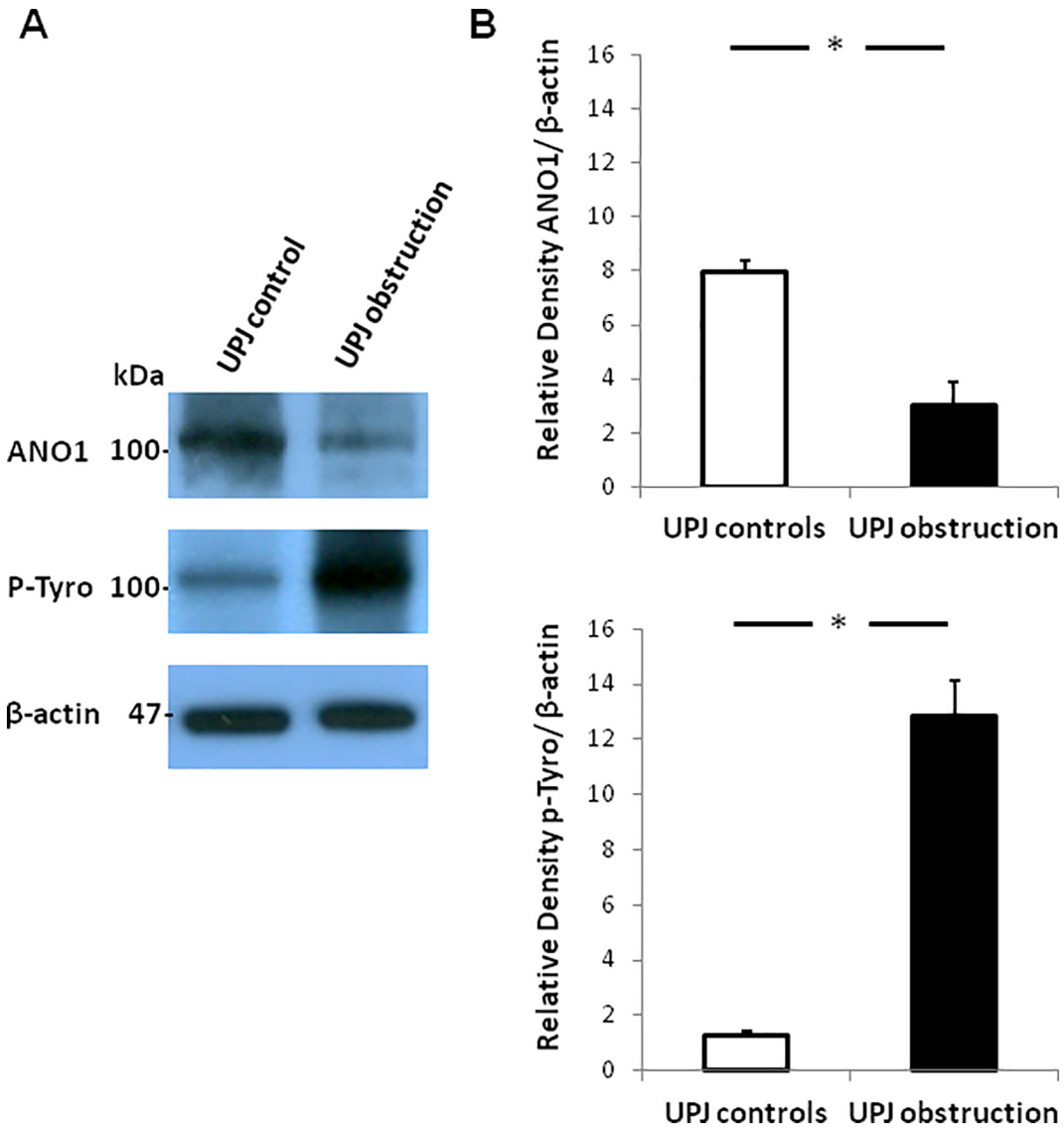

Fig. 2. Protein levels of ANO1 and tyrosine phosphorylation status in UPJ controls and UPJ obstruction. Western blotting showed markedly decreased ANO1 expression in UPJ obstruction compared to controls. Tyrosine phosphorylation was increased in UPJ obstruction compared to controls. The control peptide β-actin was similar in control and UPJ specimens **(A)**. Densitometry analysis of western blots showing a semiquantitative decrease in relative protein levels of ANO1 and an increased tyrosine phosphorylation in UPJ obstruction compared to controls **(B)**. Results are presented as mean ± SEM. (* $p = 0.02$).

between UPJ obstruction and controls were determined by a Mann Whitney U-test as the data deviated from normal distribution. A p-value of <0.05 was considered statistically significant.

2. Results

2.1. Relative mRNA expression levels of ANO1 in the human UPJ

Relative RNA expression levels of ANO1, analyzed by qRT-PCR, showed a significantly decreased gene expression of ANO1 in UPJ obstruction (0.045 ± 0.008) compared to UPJ controls (0.094 ± 0.020) (*$p = 0.016$) (Fig. 1).

2.2. Western blot

The ANO1 antibody detected a protein band of 115 kDa, the predicted molecular mass of ANO1 channels. Western blotting revealed that ANO1 protein expression was decreased in UPJ obstruction compared to controls. Furthermore, tyrosine phosphorylation was markedly increased in UPJ obstruction compared to controls (Fig. 2). Densitometry analysis confirmed a semiquantitative decrease of ANO1 ($p = 0.02$) and an increase of p-Tyro ($p = 0.02$) in UPJ obstruction compared to controls (Fig. 2). Although the methodology used does not allow to determine unequivocally whether the phosphorylated protein is indeed ANO1, as the antibody will detect any phosphotyrosine, the fact that the alterations were seen at the same band is at least indicative of a protein with the same size.

2.3. Immunofluorescence double staining and confocal microscopy

To assess whether ANO1 positive cells were structurally associated with SMCs, UPJ samples were colabeled with ANO1 antibody and Phalloidin which labels filamentous actin. Confocal-immunofluorescence revealed that ANO1 was expressed in phalloidin-positive SMCs and urothelial cells. Negative controls without a primary antibody showed no cell specific staining (data not shown). There was a strong signal observed in SMCs in both UPJ obstruction and controls (Fig. 3).

We performed double labeling immunohistochemistry to examine whether c-kit positive cells were colocalized with ANO1-positive cells.

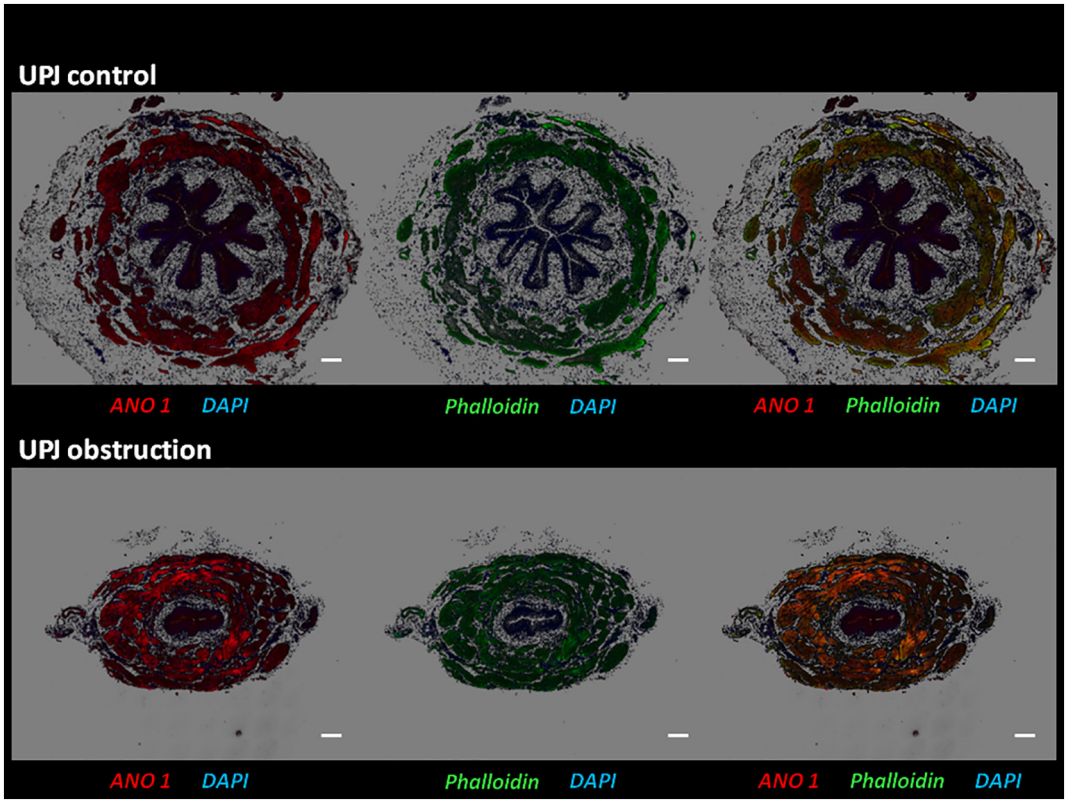

Fig. 3. Immunofluorescent double staining of ANO1 protein (red), Phalloidin (green) and overlay. Nuclei were stained with DAPI (blue). In the UPJ, ANO1 was expressed in Phalloidin-positive cells. Alpha blend projection is shown. Bar = 200 μm.

ANO1 positive cells were distinct from c-kit-positive interstitial Cajal-like cells (IC-LCs) (Fig. 4). Representative images using alpha blend projection are shown [9].

3. Discussion

It is well recognized that the antegrade transport of urine from the kidney through the ureter into the bladder occurs via propagating contractions of SMCs [3]. Experimental models have shown that impaired muscle cell differentiation can lead to functional obstruction and hydronephrosis. Although the molecular mechanisms underlying SMC maldevelopment are still largely unknown this seems, to date, the most probable cause of UPJ obstruction [10].

Functional studies of SMCs have shown that CaCCs are important in the mechanism of signal amplification leading to cell contraction [11]. CaCCs not only play a role in the regulation of smooth muscle contraction but also mediate essential physiological functions such as epithelial secretion, and control of neuronal and cardiac excitability [12,13] [14,15].

Since the identification of ANO1 as a CaCC, an increasing number of studies have reported on the essential role of ANO1 in various epithelial tissues, neuronal cells and receptors, visceral and vascular smooth muscles [16]. In mice, ANO1 has been found to be expressed in airway SMCs and in some parts of the reproductive system (i.e. oviduct, epididymis) and urethra [4,11]. More recently, ANO1 has also been documented in the rat bladder [5] and in prostrate epithelial cells [17]. While ANO1 is

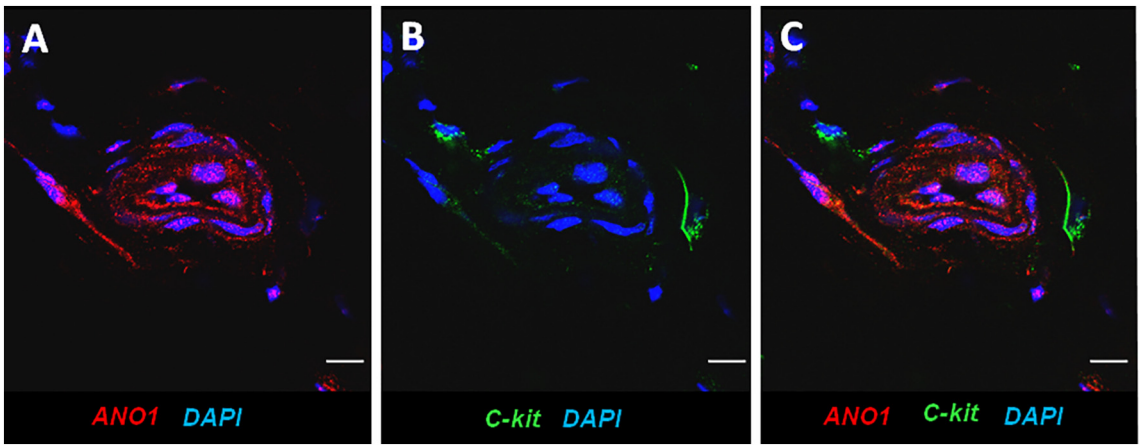

Fig. 4. Immunofluorescent double staining of ANO1 (red) (A), c-kit (green) (B) and overlay (C). Nuclei were stained with DAPI (blue). ANO1 positive cells were distinct from c-kit positive IC-LCs. Bar = 10 μm.

reported to be absent from SMCs in the gastrointestinal tract, it has been localized in interstitial cells of Cajal which are thought to mediate autorhythmicity and neurotransmission [4]. In the upper urinary tract IC-LCs are thought to play a similar role by coordinating pyeloureteral peristalsis. The identification of IC-LCs was facilitated by the discovery that the tyrosine kinase receptor c-kit is specifically expressed on their cell surface, allowing IC-LCs labeling with antibodies to the protooncogene c-kit.

Ion channels are targets of many intracellular signaling pathways, including protein phosphorylation and dephosphorylation. These processes can modify channel activity and dramatically alter electrophysiological properties on both excitable and nonexcitable cells [7].

Although ANO1 carries multiple predicted phosphorylation sites for Ca^{2+} dependent kinases such as Ca^{2+}/calmodulin-dependent protein kinase (CAMK), protein kinase C and protein kinase A [18], none of these kinases seem to be relevant for gating ANO1. Thus, although the presence of calmodulin and ATP appears important for activation of ANO1, calmodulin dependent kinase (CAMKII) is not required [16]. However, CAKMII phosphorylates serine and threonine residues [19]. An emerging body of evidence suggests that various ion channels are also regulated by phosphorylation on tyrosine residues such as L-type Ca^{2+} channels in vascular smooth muscles [7].

The findings of our study demonstrate, for the first time, the expression of ANO1 in the human upper urinary tract. ANO1 was localized to SMCs and urothelium but not to the IC-LCs. These results strengthen the findings of Sancho et al. who were able to demonstrate ANO1 expression in urethral SMCs and urothelium of mice, sheep and rat but not in IC-LCs [4]. In addition, our results show that expression of ANO1 is decreased in UPJ obstruction. Western blot analysis revealed that the relative density of ANO1 was decreased in UPJ obstruction compared to controls indicating a lower density of ANO1 per cell.

Furthermore, not only the expression but also the function of ANO1 in SMCs has been shown to be altered under pathological conditions such as hypertension, asthma like-conditions and chronic hypoxia [6]. Our study confirmed that tyrosine phosphorylation is altered in UPJ obstruction compared to controls. The alterations in activity may lead to aberrant smooth muscle contraction in UPJ obstruction, leading to a failure of peristalsis. However, we did not know the physiological role of tyrosine phosphorylation or its impact on channel function. Although there are alterations in ANO1 and in phosphotyrosine in UPJO, it does not necessarily follow that ANO1 tyrosine phosphorylation is altered. Further functional studies are needed to confirm the pathological significance in this urological disease.

Conflict of interest

The authors declare that they have no conflict of interest.

Funding

The authors have no financial relationships relevant to this article to disclose.

Ethical approval

This study was approved by the Ethics (Medical Research) Committee, Our Lady's Children's Hospital, Dublin (Ref. GEN/200/11).

Disclosure

All the authors declare no competing interests.

Acknowledgments

We thank Mr. Feargal Quinn, Mr. Sri Paran, Mr. Brice Antao, Dr. Michael McDermott and Prof. Maureen O'Sullivan, for their assistance in sample collection.

References

[1] Lang RJ, Davidson ME, Exintaris B. Pyeloureteral motility and ureteral peristalsis: essential role of sensory nerves and endogenous prostaglandins. Exp Physiol 2002; 87:129–46.
[2] Hosgor M, Karaca I, Ulukus C, et al. Structural changes of smooth muscle in congenital ureteropelvic junction obstruction. J Pediatr Surg 2005;40:1632–6.
[3] Iqbal J, Tonta MA, Mitsui R, et al. Potassium and ANO1/ TMEM16A chloride channel profiles distinguish atypical and typical smooth muscle cells from interstitial cells in the mouse renal pelvis. Br J Pharmacol 2012;165:2389–408.
[4] Sancho M, Garcia-Pascual A, Triguero D. Presence of the Ca2+-activated chloride channel anoctamin 1 in the urethra and its role in excitatory neurotransmission. Am J Physiol Renal Physiol 2012;302:F390–400.
[5] Bijos DA, Drake MJ, Vahabi B. Anoctamin-1 in the juvenile rat urinary bladder. PloS one 2014;9:e106190.
[6] Pedemonte N, Galietta LJ. Structure and function of TMEM16 proteins (anoctamins). Physiol Rev 2014;94:419–59.
[7] Davis MJ, Wu X, Nurkiewicz TR, et al. Regulation of ion channels by protein tyrosine phosphorylation. Am J Physiol Heart Circ Physiol 2001;281:H1835–62.
[8] Angermann JE, Sanguinetti AR, Kenyon JL, et al. Mechanism of the inhibition of Ca2+-activated Cl- currents by phosphorylation in pulmonary arterial smooth muscle cells. J Gen Physiol 2006;128:73–87.
[9] White NS. Visualization system for multidimensional microscopy images. In: Pawley JB, editor. In handbook of biological confocal microscopy. 3rd ed. New York: Springer; 2006. p. 280–91.
[10] Klein J, Gonzalez J, Miravete M, et al. Congenital ureteropelvic junction obstruction: human disease and animal models. Int J Exp Pathol 2011;92:168–92.
[11] Ferrera L, Caputo A, Galietta LJ. TMEM16A protein: a new identity for Ca(2+)-dependent Cl(−) channels. Physiology (Bethesda) 2010; 25: 357–63.
[12] Huang F, Rock JR, Harfe BD, et al. Studies on expression and function of the TMEM16A calcium-activated chloride channel. Proc Natl Acad Sci U S A 2009;106: 21413–8.
[13] Caputo A, Caci E, Ferrera L, et al. TMEM16A, a membrane protein associated with calcium-dependent chloride channel activity. Science 2008;322:590–4.
[14] Duran C, Hartzell HC. Physiological roles and diseases of Tmem16/Anoctamin proteins: are they all chloride channels? Acta Pharmacol Sin 2011;32: 685–92.
[15] Galietta LJ. The TMEM16 protein family: a new class of chloride channels? Biophys J 2009;97:3047–53.
[16] Kunzelmann K, Tian Y, Martins JR, et al. Anoctamins. Pflugers Arch 2011;462: 195–208.
[17] Cha JY, Wee J, Jung J, et al. Anoctamin 1 (TMEM16A) is essential for testosterone-induced prostate hyperplasia. Proc Natl Acad Sci U S A 2015;112:9722–7.
[18] Kunzelmann K, Kongsuphol P, Aldehni F, et al. Bestrophin and TMEM16-Ca(2+) activated Cl(−) channels with different functions. Cell Calcium 2009;46: 233–41.
[19] Greenwood IA, Ledoux J, Leblanc N. Differential regulation of Ca(2+)-activated Cl(−) currents in rabbit arterial and portal vein smooth muscle cells by Ca(2+)-calmodulin-dependent kinase. J Physiol 2001;534:395–408.